Journal of Medicinal Chemistry

Article

pubs.acs.org/jmc

Discovery of CREBBP Bromodomain Inhibitors by High-Throughput Docking and Hit Optimization Guided by Molecular Dynamics

Min Xu,[†] Andrea Unzue,[‡] Jing Dong,[†] Dimitrios Spiliotopoulos,[†] Cristina Nevado,*[,‡] and Amedeo Caflisch*[,†]

[†]Department of Biochemistry, University of Zürich, Winterthurerstrasse 190, CH-8057, Zürich, Switzerland

[‡]Department of Chemistry, University of Zürich, Winterthurerstrasse 190, CH-8057, Zürich, Switzerland

Supporting Information

ABSTRACT: We have identified two chemotypes of CREBBP bromodomain ligands by fragment-based high-throughput docking. Only 17 molecules from the original library of two-million compounds were tested in vitro. Optimization of the two low-micromolar hits, the 4-acylpyrrole **1** and acylbenzene **9**, was driven by molecular dynamics results which suggested improvement of the polar interactions with the Arg1173 side chain at the rim of the binding site. The synthesis of only two derivatives of **1** yielded the 4-acylpyrrole **6** which shows a single-digit micromolar affinity for the CREBBP bromodomain and a ligand efficiency of 0.34 kcal/mol per non-hydrogen atom. Optimization of the acylbenzene hit **9** resulted in a series of derivatives with nanomolar potencies, good ligand efficiency and selectivity (see Unzue, A.; Xu, M.; Dong, J.; Wiedmer, L.; Spiliotopoulos, D.; Caflisch, A.; Nevado, C. Fragment-Based Design of Selective Nanomolar Ligands of the CREBBP Bromodomain. *J. Med. Chem.* **2015**, DOI: 10.1021/acs.jmedchem.5b00172). The in silico predicted binding mode of the acylbenzene derivative **10** was validated by solving the structure of the complex with the CREBBP bromodomain.

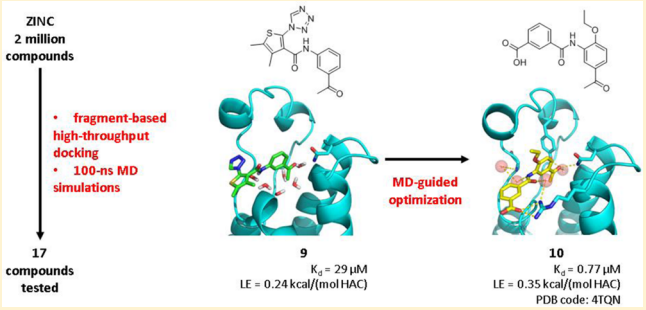

INTRODUCTION

Bromodomains are α-helical modules of about 110 residues that bind the acetylated side chain of lysine most notably (but not exclusively) in histone proteins.[1] Bromodomain-containing proteins have up to six of these modules. Some of these proteins play a crucial role in numerous cellular processes, such as gene regulation.[2] The three-dimensional structures of most of the 61 human bromodomains have been solved by X-ray crystallography[3] and in a few cases by NMR spectroscopy.[4]

Small molecules inhibiting CREBBP bromodomain acetyllysine-binding activity have been identified in the last years (Figure 1). Zhou et al. used NMR spectroscopy (the $^{1}H-^{15}N$ HSQC spectra) to screen a small compound library and were the first to identify two compounds that block the interaction between p53 and KAc382-CREBBP at 100 and 50 μM, respectively (compounds **A** and **B** in Figure 1).[4a] The same group identified ischemin, which has an IC_{50} of 5 μM for the CREBBP bromodomain (**C**, Figure 1),[4b] and synthesized a p53-like cyclic peptide that binds the CREBBP bromodomain with an IC_{50} of 5 μM.[5] The identification of *N*-methyl-2-pyrrolidone as a weak antagonist of acetylated peptide-binding by the CREBBP bromodomain (**D**, Figure 1)[6] ignited studies on methyl-bearing heterocycles by Hewings and co-workers, who developed substituted 3,5-dimethylisoxazoles compounds targeting BET bromodomains, and a poorly selective CREBBP bromodomain inhibitor (**E**, Figure 1).[7] In a study that focused on 40 crystal structures of the N-terminal bromodomain of BRD2 in the complex with rigid fragments, Chung et al. disclosed also the crystal structure of the complex of the CREBBP bromodomain and paracetamol (**F**, Figure 1).[8] Hay and collaborators described some nonselective CREBBP ligands while aiming to identify BET inhibitors (**G**, Figure 1).[9] Another 3,5-dimethylisoxazole derivative potently and selectively binding the CREBBP bromodomain (called SGC-CBP30) has been reported recently (**H**, Figure 1).[10] The SGC has also reported the development of a nanomolar CREBBP bromodomain inhibitor, I-CBP112, which exhibits weak binding activity toward the BET bromodomains (**I**, Figure 1).[11] Rooney and co-workers developed a dihydroquinoxalinone series ultimately leading to a modestly selective nanomolar CREBBP bromodomain inhibitor (**J**, Figure 1).[12] A series of [1,2,4]triazolo[4,3-*a*]phthalazines was shown recently to bind unselectively to diverse bromodomains including CREBBP (**K**, Figure 1).[13]

To identify small molecules that bind selectively to the CREBBP bromodomain, we have performed in silico screening with two crystal structures of this target. ALTA (anchor-based library tailoring),[14] a four-step procedure developed in house for docking large libraries of compounds, was used for virtual

Special Issue: Epigenetics

Received: January 29, 2015
Published: June 30, 2015

DOI: 10.1021/acs.jmedchem.5b00171
J. Med. Chem. 2016, 59, 1340−1349

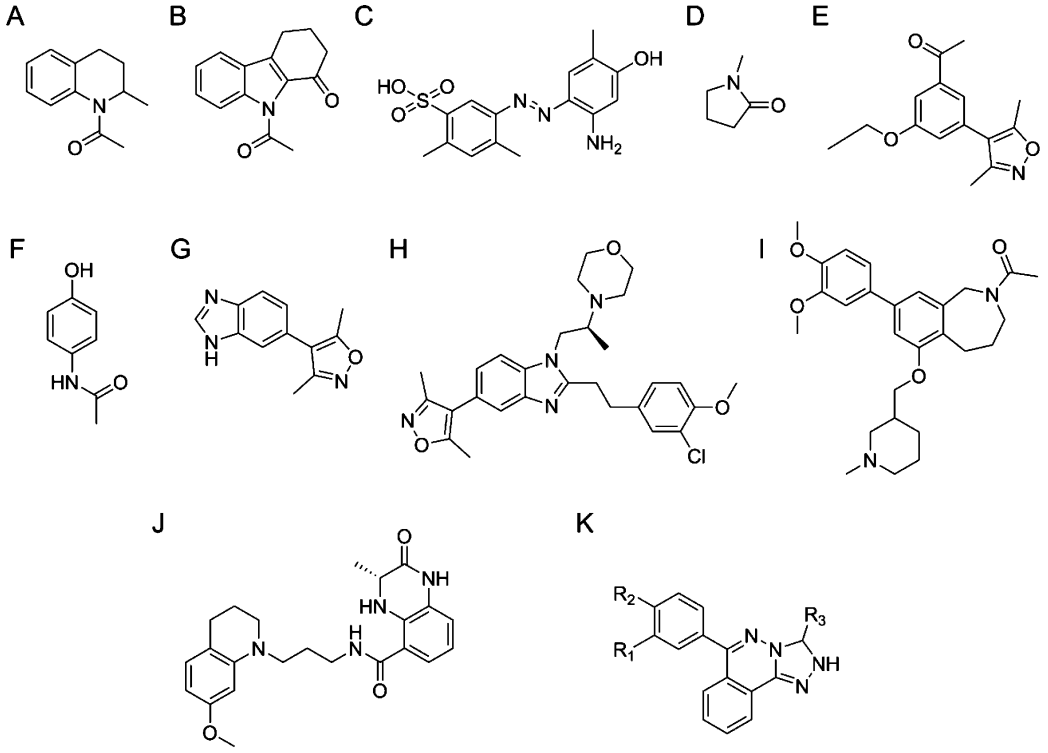

Figure 1. Known CREBBP inhibitors reported in the literature. Compounds **B**, **C**, **D**, **E**, **H**, **I**, and **J** can be found in complex with the CREBBP bromodomain in the PDB files 2D82, 2L84, 3P1D, 3SVH, 4NR7, 4NR6 and 4NYX, respectively.

screening. In the first step, the molecules are decomposed into rigid fragments by an algorithm that cuts at rotatable bonds.[15] In the second step, the fragments are docked and ranked using an energy evaluation that takes into account solvation effects in the continuum dielectric approximation.[16] Third, the procedure identifies the molecules that contain at least one of the top ranking fragments. The final step consists of the flexible docking of the retrieved molecules followed by energy minimization and evaluation of desolvation penalties.

Here we report on the in silico discovery by the ALTA procedure of two hits (compounds **1** and **9**) for the CREBBP bromodomain. To the best of our knowledge, this is the first in silico screening that targets the CREBBP bromodomain. Multiple molecular dynamics (MD) runs with explicit solvent were carried out to further validate the binding mode suggested by docking and guide chemical synthesis for hit optimization. The synthesis of only two derivatives of the 4-acylpyrrole hit **1** resulted in a single-digit micromolar ligand of the CREBBP bromodomain with excellent ligand efficiency. The optimization of the acylbenzene hit **9** is described in detail in ref 17.

DOCKING RESULTS

Docking of Fragments. The ALTA procedure started with the decomposition of the nearly two million compounds in the ZINC leads-now library (version of October 2012) by the DAIM program[15] (Figure 2). To target the conserved Asn involved in binding the natural ligand acetyllysine (numbered 1168 in the PDB structures 3P1C and 3SVH), only fragments with a hydrogen bond donor or acceptor were kept. Although the natural ligand (acetyllysine) acts as hydrogen bond acceptor for the amide side chain of the conserved Asn, it was decided to also consider fragments with a hydrogen bond donor because our previous MD simulations revealed that the amide of the Asn side chain occupies both possible orientations (Figure 2 of ref 18). Further removal of fragments without a ring yielded a set of 106 534 fragments.

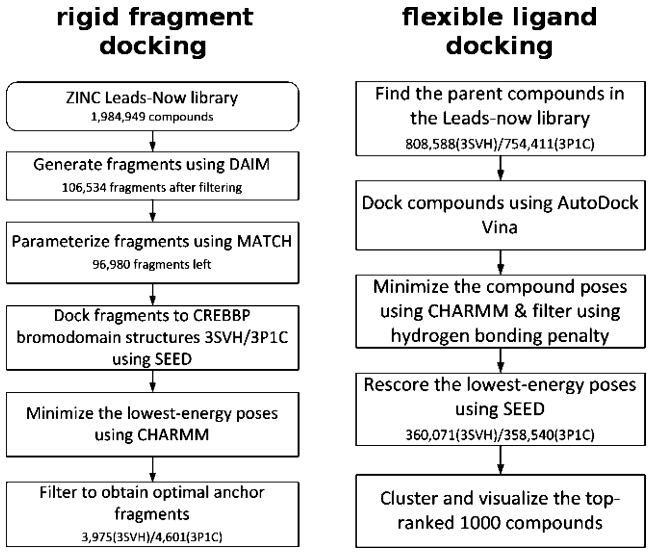

Figure 2. (Left) Flowchart of fragment docking which is the initial phase of the ALTA (anchor-based library tailoring) procedure.[14a] The program DAIM automatically decomposes molecules into fragments by cutting at rotatable bonds.[15] The fragment-docking tool SEED[16] required about 5 s per fragment on a single core of an i7 CPU at 2.8 GHz. CHARMM[20] minimization of the fragment with rigid CREBBP took about 2 s per fragment. (Right) Flowchart of flexible ligand docking which is the second phase of the ALTA procedure. Flexible ligand docking by AutoDock Vina required about 1 min per compound.

The X-ray structures of the CREBBP bromodomain in complex with the natural ligand acetyllysine (PDB code 3P1C)

DOI: 10.1021/acs.jmedchem.5b00171
J. Med. Chem. 2016, 59, 1340−1349

and the synthetic ligand 3,5-dimethylisoxazole (3SVH) show different orientations of the side chain of the so-called gatekeeper residue, Val1174 (Figure 3).[19] Furthermore, the

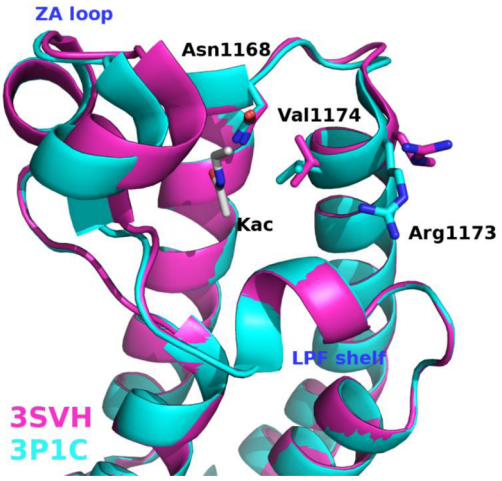

Figure 3. Overlap of the two crystal structures of the CREBBP bromodomain used for docking. The helical secondary structure is shown by ribbons. The conserved Asn1168 and the residues with variable side chain orientation that are mentioned in the text are shown in sticks. The physiological ligand (acetylated lysine) is shown as sticks (carbon atoms in gray).

solvent-exposed side chain of Arg1173 seems very flexible in the two crystallographic structures. In 3P1C, it is just above the Leu-Pro-Phe segment (called LPF, in the following; this tripeptide stretch corresponds to the WPF segment in most bromodomains). On the contrary, in 3SVH the Arg1173 guanidinium points outward (Figure 3). Given these differences, it was decided to use both structures for docking. After the preparation of the two protein structures (see Experimental Section), the fragment library was docked into the binding pocket by the program SEED.[16]

Two additional filters were applied to reduce the number of docked fragments to about 4000 for each of the two CREBBP structures (Figure 2, left): (a) SEED total energy efficiency more favorable than −0.125 kcal mol^{-1} g^{-1} and (b) hydrogen bonding penalty of less than or equal to 1.[21] These criteria efficiently enriched the fragments involved in hydrogen bond(s) with the Asn1168 side chain, a key interaction present in the complex of the natural ligand with CREBBP (Figure 3). Quantitatively, after filtering there were 91% and 82% of fragments forming at least one hydrogen bond with the Asn1168 side chain for 3SVH and 3P1C, respectively, while before filtering there were 33% and 41%, respectively.

To assess the predictive ability of the procedure used for fragment ranking, six fragments from known inhibitors were also docked by SEED (Figure 4). Importantly, the pose of these fragments predicted by SEED matches within 1 Å the binding mode observed in the crystal structures.

For each of the two crystal structures used for docking, the receiver-operator characteristic (ROC) plot generated using about 100 000 fragments with optimal SEED energy efficiency (considered as false positives) and six fragments from known inhibitors (true positives) gives an area under the curve of 0.985. The individual ranks of the six known fragments are listed in Figure 4. Thus, the very large area under the curve and the good ranks of the fragments from known inhibitors provide

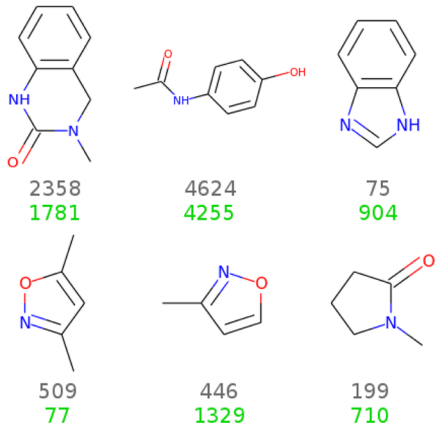

Figure 4. Validation of the filtering and ranking procedures. The figure shows the six fragments from known CREBBP and BET bromodomain inhibitors[22] that were used as validation set, i.e., considered as true positives. The two integers below each fragment are their ranks among the 96 724 putatively inactive fragments docked into the 31PC structure (gray) and the 100 027 putatively inactive fragments docked into 3SVH (green), respectively.

evidence that the filtering and ranking procedure is able to prioritize true positives.

Docking of Compounds with Optimal Anchor Fragments. About 4000 fragments were used to retrieve the molecules in the ZINC library which they originated from (called parent compounds hereafter). There were 808 588 (3SVH)/754 411 (3P1C) parent compounds in total and for each of them at most 15 poses were generated by AutoDock Vina.[23] All the poses were then minimized, filtered, and rescored using the SEED total energy (Figure 2, right). In the end, the top-ranking poses of 1000 compounds according to the SEED total energy were chosen and analyzed. They were clustered based on the functional groups interacting with the conserved Asn1168, which in the following is referred to as the "head group". The chemical space of the head groups was rather condensed (Figure 5). Thus, only 20 compounds (representing all of the head groups) were chosen for further investigation by MD simulations to verify the stability of the binding mode.

This analysis ruled out three compounds, as they moved out of the binding site within 100 ns (Figure S1 in Supporting Information). The remaining 17 molecules were purchased and tested by a competition binding assay (BROMOScan at DiscoveRx).[24] Two of these compounds (**1** and **9**), both featuring an acetylated aromatic ring, showed an equilibrium dissociation constant (K_d) in the low μM range (Figure 6, Figures S2 and S5). Note that the acylaryl moieties of compounds **1** and **9** do not appear in Figure 5 because they were not among the most frequent in the 1000 top ranked compounds. Nonetheless, the aforementioned clustering and MD simulations were able to identify them.

EXPERIMENTAL RESULTS

Optimization of 4-Acylpyrrole Hit 1 Guided by MD Simulation Results. The binding mode of compound **1** obtained by rigid-protein docking into CREBBP bromodomain indicates that its acyl group acts as hydrogen bond acceptor for the side chain of the conserved Asn1168 (Figure S2A). Thus, five additional commercially available 4-acylpyrrole derivatives

DOI: 10.1021/acs.jmedchem.5b00171
J. Med. Chem. 2016, 59, 1340−1349

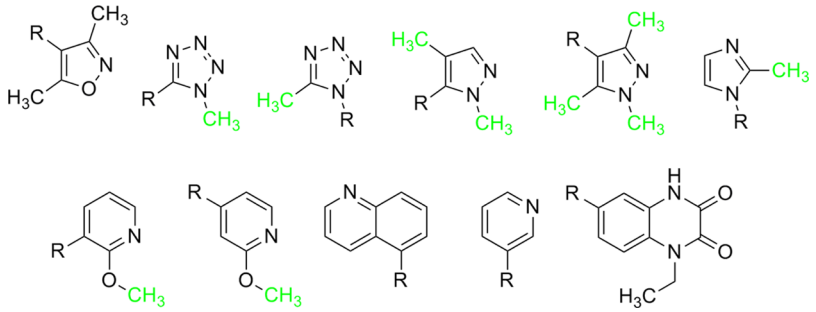

Figure 5. Most frequent anchor fragments in the 1000 top ranked compounds. The methyl groups in green are H atoms in some of the compounds.

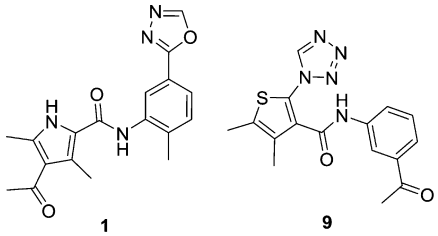

Figure 6. CREBBP bromodomain hits identified by the fragment-based ALTA procedure. In the binding mode predicted by docking the acetyl group accepts a hydrogen bond from the side chain of Asn1168. K_d values for the CREBBP bromodomain were measured by the competition binding assay[24] (Figure S5).

were tested. Among these, compounds **2**, **3**, and **4** showed activity at 50 μM in a competition binding assay (Table 1).[24]

Next, we analyzed the predicted binding modes of compounds **1**–**4**, which share the presence of an amide as a linker connecting the 4-acylpyrrole (the compounds' "head group") with a partially exposed moiety (called "tail group" henceforth). Their binding poses, as predicted by docking, are overall similar (Figure S3). The acyl oxygen is involved as acceptor in a hydrogen bond with the amide side chain of Asn1168. The two alkyl substituents on the pyrrole ring further strengthen the binding mode by van der Waals interactions with the side chains of Leu1120 on the ZA loop and Val1174. The linker amide establishes a hydrogen bond with one of the structured water molecules while maintaining the conserved water molecule network within the binding site. Interestingly,

Table 1. Experimental Validation of 4-Acylpyrroles Binding to the CREBBP Bromodomain[e]

Compound	2D structure	Thermal shift (°C)[a]	K_d [%Ctrl @50 μM][b]	IC_{50}[c]	Ligand efficiency[d]
1	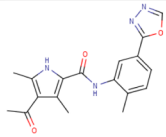	0.3	13 μM [9%]	> 100 μM	0.27
2	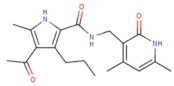	0.3	[3%]	ND	ND
3	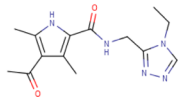	1.3	[5%]	ND	ND
4	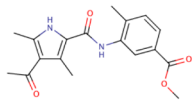	ND	[20%]	ND	ND
5	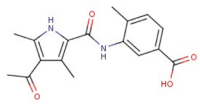	1.4	ND	> 10 μM	ND
6	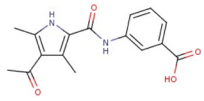	2.3	4.2 μM	1.5 μM	0.34, 0.37

[a]The thermal shift experiments were carried out at a protein concentration of 2 μM and a ligand concentration of 100 μM. At least 16 measurements were acquired for each compound. All standard error values were below 0.2 °C. [b]Dissociation constants were measured by a competition binding assay (Figure S5).[24] The percentage of the measured signal at an inhibitor concentration of 50 μM with respect to the negative control DMSO is given in brackets with lower values indicating stronger binding. Measurements at each dose were done in duplicate. [c]The IC_{50} values were determined by a TR-FRET assay (see Supporting Information). The values are averages of duplicate dose–response measurements. Compound **1** is a false negative in the TR-FRET assay. [d]The ligand efficiency has units of kcal/(mol HAC) where HAC is the heavy atom count. [e]Hit **1** was identified by the ALTA procedure. Compounds **2**–**4** were identified by substructure search, and compounds **5** and **6** were synthesized (see Scheme 1). ND: not determined.

DOI: 10.1021/acs.jmedchem.5b00171
J. Med. Chem. 2016, 59, 1340–1349

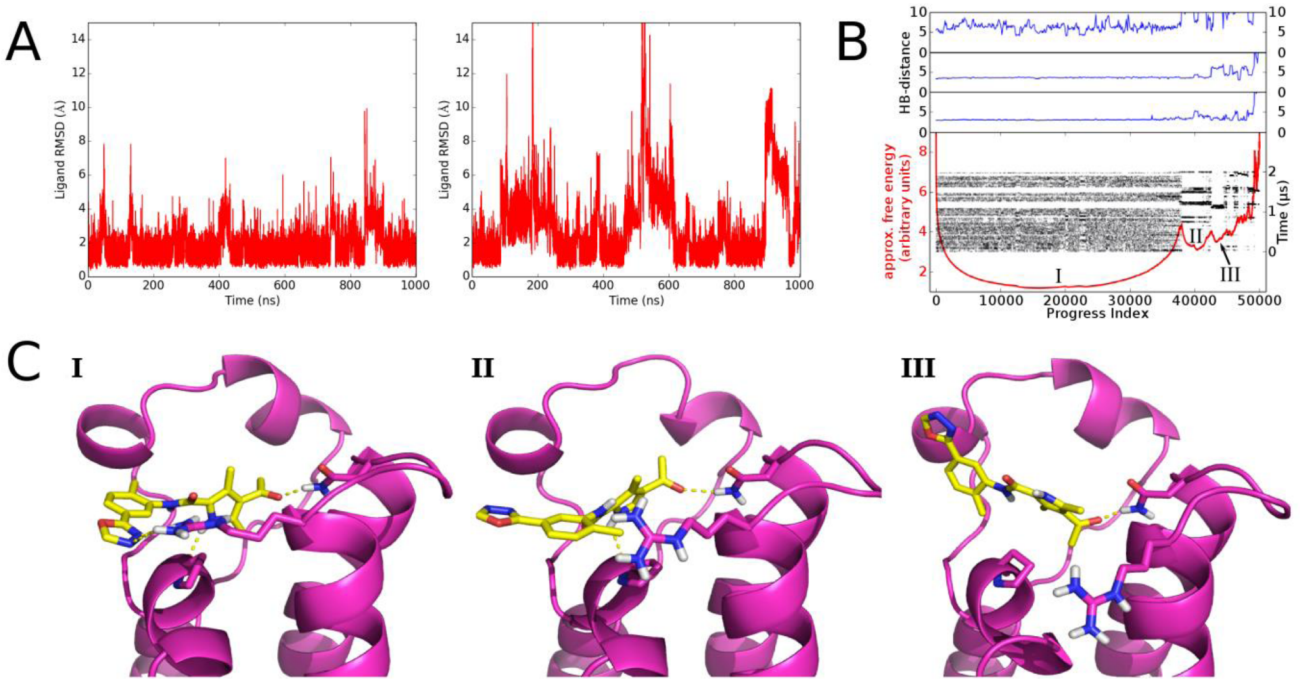

Figure 7. Structural stability and multiple binding modes of compound **1** in complex with the CREBBP bromodomain. (A) Two independent MD runs were started from the binding mode obtained by docking using different initial velocities. The 100 000 snapshots (saved every 20 ps) were overlapped using the Cα atoms of the helical segments of the CREBBP bromodomain, and the time series of the RMSD of the heavy atoms of compound **1** was calculated. (B) MD simulations suggest multiple binding modes for compound **1**. The free-energy profile[27] of the binding of compound **1** to the CREBBP bromodomain (red curve) is shown together with the trace of the temporal evolution of the system during the 2 μs MD sampling (black dots). The dynamical trace illustrates the transitions between free-energy basins.[28] The free-energy profile is annotated with the following intermolecular hydrogen bond distances (blue): between the oxadiazole and the guanidinium of Arg1173 (top), the NH of the pyrrole and the backbone carbonyl of Pro1110 (middle), and the acetyl oxygen and the amide of the conserved Asn1168 (bottom). The distances were calculated between donor and acceptor atoms, and they were averaged every 4 ns. The two hydrogen bonds involving the 4-acylpyrrole are stable, while the hydrogen bond with the Arg1173 is unstable. (C) The most populated binding mode and two alternative binding modes of compound **1** are indicated with Roman numerals (I, II, and III, respectively).

the pyrrole nitrogen acts as a hydrogen donor to the carbonyl of Pro1110 (in the LPF segment), an interaction first observed in MD simulations of the CREBBP and other bromodomains with the natural acetyllysine ligand.[25] It is interesting to note that this MD simulation result was confirmed by two reports on inhibitors forming a similar hydrogen bond to the conserved proline of various bromodomains.[26]

The partially exposed tail group of compound **1** is a 1,3,4-oxadiazole ring, which is in van der Waals contact with the Pro1110 side chain in the LPF shelf. Compound **1** is also involved in favorable polar interactions with the guanidinium group of Arg1173. This positively charged residue is unique to CREBBP (and its paralogue EP300), and thus, interactions with its side chain are likely to result in selectivity toward CREBBP (cf. also refs 4b, 7, 12, and 17). On the contrary, the tail moieties of compounds **2** and **3** (a 4,6-dimethylpyridin-2(1*H*)-one and a 4-ethyl-4*H*-1,2,4-triazole, respectively) are predicted to insert into the so-called ZA channel, which is hydrophobic in the CREBBP bromodomain.

Given the promising K_d value of compound **1** (Figure 6 and Table 1), we aimed to further validate its predicted binding mode into CREBBP by carrying out explicit solvent MD simulations of the complex. Two independent 1 μs MD runs were launched with different initial assignment of the random velocities. The time series of the root-mean-square deviation (RMSD) of compound **1** show that the binding mode is overall stable, although deviations of different magnitude are observed in the two MD runs (Figure 7A). The free-energy profile analysis of the cumulated MD sampling reveals three sub-basins corresponding to three main binding modes, respectively (Figure 7B,C). The largest basin (i.e., pose I) contains about 75% of the 50 000 MD snapshots (saved along 2 μs of total MD sampling) and corresponds to the binding mode predicted by automatic docking. Within this basin, the two hydrogen bonds formed by the 4-acylpyrrole with the conserved Asn and Pro residues are stable. In addition, the 1,3,4-oxadiazole forms a stable interaction with the LPF segment. On the other hand, the direct hydrogen bonds between the 1,3,4-oxadiazole nitrogen atoms and the guanidinium group of Arg1173 are sporadic and show frequent fluctuations during which a single water molecule inserts itself to form a water-mediated hydrogen bond. Quantitatively, the shortest distance between any of the two oxadiazole nitrogen atoms of compound **1** and any NH atoms of the Arg1173 guanidinium is shorter than 3.5 and 5 Å only in 17% and 33% of the MD snapshots, respectively (Figure 7B).

The second largest free-energy basin is sampled in both simulations and is similar to the binding pose predicted by docking of compounds **2** and **3** (compare pose II in Figure 7C to Figure S3). In this alternative pose the 4-acylpyrrole group is anchored in the acetyllysine binding pocket, whereas the 1,3,4-oxadiazole group is in a different orientation with respect to the previous conformation, as it flips toward the ZA channel on the other side of the binding site.

Finally, a third binding conformation was revealed by the free-energy profile (pose III in Figure 7C) with the displace-

DOI: 10.1021/acs.jmedchem.5b00171
J. Med. Chem. 2016, 59, 1340−1349

Scheme 1[a]

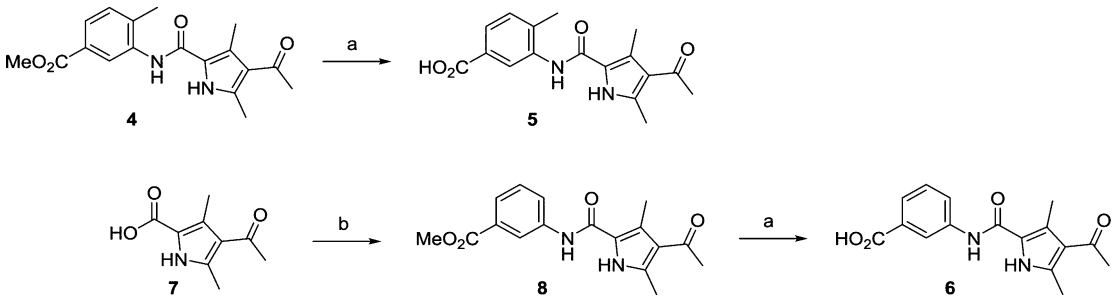

[a]Reagents and conditions: (a) 1 M LiOH, THF, 25 °C, 3−5 h, 59−65%; (b) $(COCl)_2$, DMF, DCM, 30 min at 0 °C and 1 h at 25 °C, then methyl 3-aminobenzoate, Et_3N, DMAP, 25 °C, 12 h, 53%.

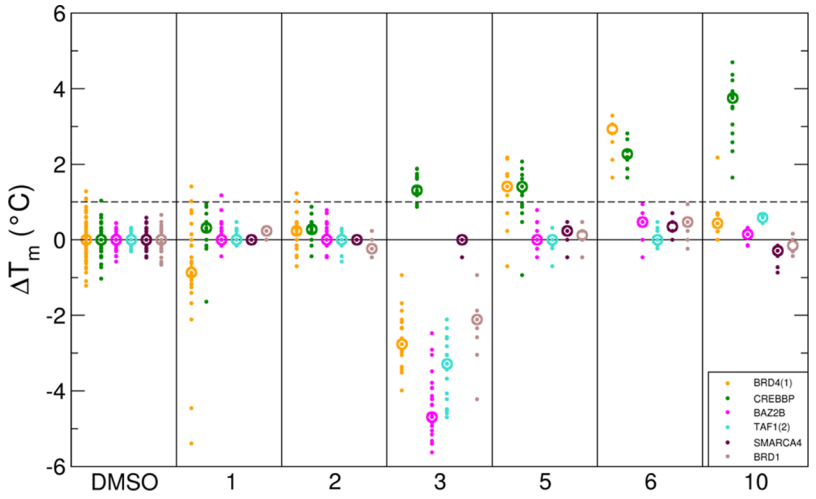

Figure 8. Thermal shift values (ΔT_m) measured in a panel of six bromodomains belonging to six different subfamilies. The plot shows for each compound and each bromodomain the independent measurements (dots) and median value (circle). The dashed line at 1 °C is an arbitrary threshold. The compounds are sorted by compound number along the *x*-axis, and different colors are used for different bromodomains (legend).

Table 2. Experimental Validation of Acylbenzenes Binding to the CREBBP Bromodomain and Selectivity versus BRD4(1) Bromodomain[d]

	Compound	Kd (μM)[a]	LE[b]	Selectivity CREBBP vs. BRD4(1)[c]
9	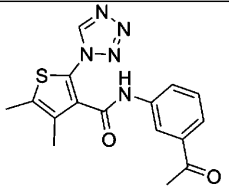	29	0.24	ND
10	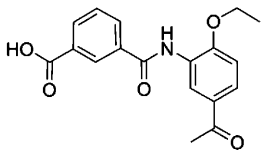	0.77	0.35	>65

[a]K_d values for the CREBBP bromodomain were measured by the competition binding assay[24] (Figure S5). [b]The ligand efficiency has units of kcal/(mol HAC) where HAC is the heavy atom count. [c]Ratio of the K_d values for BRD4(1) and CREBBP bromodomains as measured by the competition binding assay. ND: not determined. [d]Hit **9** was identified by the ALTA procedure, while compound **10** was synthesized.

ment of the tail group away from the LPF segment and the rotation of the acyl group of the pyrrole, which maintains the hydrogen bond with the side chain of the conserved Asn.

The MD analysis of compound **1** suggested that a negatively charged group instead of the 1,3,4-oxadiazole ring might result in more favorable electrostatic interactions with the Arg1173 side chain and thus favor selectivity for CREBBP bromodomain over other bromodomains. Therefore, we decided to carry out a small hit optimization campaign, namely, to replace the 1,3,4-oxadiazole with a carboxylic group. To this end, we synthesized compounds **5**, **6**, and **8** (Scheme 1). Compound **8** was prepared by condensation of commercially available 4-acetyl-3,5-

DOI: 10.1021/acs.jmedchem.5b00171
J. Med. Chem. 2016, 59, 1340−1349

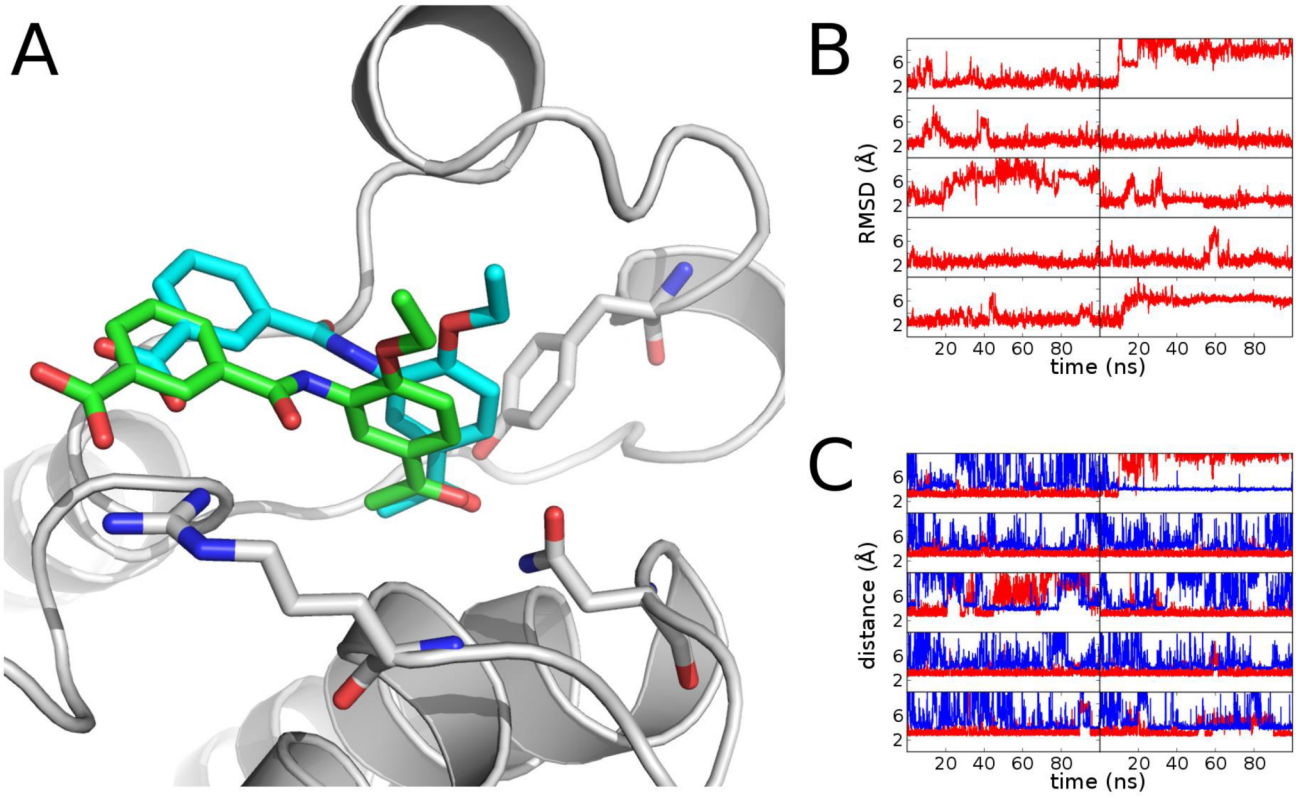

Figure 9. (A) The binding mode of compound **10** predicted by docking and MD simulations (carbon atoms in cyan) is similar to the crystal structure of the complex (carbon atoms in green, from PDB code 4TQN) except for the orientation of the amide linker. Note that both orientations of the amide linker were sampled during the MD simulations but the one observed in the crystal structure was less populated which is likely due to the fact that the MD runs were started with the wrong orientation and the length of the individual runs is too short to reach equilibrium. The crystal structure of CREBBP (gray) is rendered by a ribbon representation with relevant side chains in sticks. (B) Time series of the RMSD of compound **10** along 10 independent MD runs of 100 ns each. The RMSD values were calculated for the heavy atoms of the ligands after overlapping the Cα atoms of the helical segments of the CREBBP bromodomain. (C) Time series of the distance between the carbonyl oxygen of compound **10** and the Asn1168 side chain N atom (red), and the distance between the carboxyl carbon atom of compound **10** and Arg1173 Cζ (blue) along the trajectory.

dimethyl-1*H*-pyrrole-2-carboxylic acid **7** and methyl 3-aminobenzoate. Consequent hydrolysis (in the presence of LiOH) of the methyl ester in **8** and in the commercially available compound **4** afforded the final compounds **5** and **6** in 59% and 65% yield, respectively.

As predicted, the 4-acylpyrrole derivative **6** is more potent than the hit **1** in the competition binding assay and the TR-FRET assay (Table 1). Concerning their selectivity, compounds **5** and **6** show similar thermal shift values for CREBBP and BRD4(1) and no shift for four bromodomains belonging to other subfamilies (Figure 8).

Optimization of Acylbenzene Hit 9 and MD Simulations. Concurrent with the investigations on the 4-acylpyrrole derivatives (compounds **1**–**6**), we optimized the acylbenzene hit **9** as described in ref 17. In short, after purchasing a few commercially available derivatives of **9**, optimization by chemical synthesis guided by analysis of the docking pose resulted in compound **10**, which showed an improved potency (0.77 μM vs 29 μM) and ligand efficiency (0.35 vs 0.24 kcal/mol per non-hydrogen atom) compared to the parent compound **9**. In addition, **10** showed more than 65 times higher affinity for CREBBP than for the first bromodomain of BRD4 (Table 2, Figure S5).

The binding mode of the benzoic acid derivative **10** obtained by docking was first validated by 10 MD simulations of 100 ns each during which the direct salt bridge between the carboxyl group of **10** and the guanidinium of Arg1173 was present for about 70% of the time (up to 80% considering also a single-water bridged interaction, Figure 9B,C). The crystal structure of acylbenzene **10** in complex with the CREBBP bromodomain at 1.7 Å resolution (PDB code 4TQN, Table S1) is in line with the binding mode predicted by docking and MD simulations (Figure 9A).

CONCLUSIONS

We have identified two chemical classes of CREBBP bromodomain inhibitors by the ALTA procedure[14] for fragment-based high-throughput docking. The ranking of fragments and molecules was based on the evaluation of the binding energy using a classical force field and including the desolvation penalty calculated in the continuum electrostatics approximation. The hit rate of our in silico screening procedure was high, as two active molecules (K_d values of 13 and 29 μM for ligands **1** and **9**, respectively) were identified by testing in vitro only 17 compounds. Optimization of the two hits was guided by the results of explicit solvent MD simulations.

The 4-acylpyrrole hit **1** underwent a limited optimization because of its lack of selectivity for CREBBP, which is consistent with a recent report on the discovery of 4-acylpyrrole derivatives as BET bromodomain inhibitors.[26a] One of these BET inhibitors (called XD14) was reported to bind also to the CREBBP bromodomain with an affinity of 1.6 μM in the

DOI: 10.1021/acs.jmedchem.5b00171
J. Med. Chem. 2016, 59, 1340−1349

competition binding assay, which is similar to the one of our inhibitor **6**. Of note, our compound **6** has a heavy atom count (HAC) of 22 and thus a more favorable ligand efficiency for CREBBP (0.34 kcal/mol per HAC, Table 1) than the larger XD14 (29 HAC and 0.28 kcal/mol per HAC).

The acylbenzene hit **9** was optimized by chemical synthesis of less than 30 derivatives which are described in detail in ref 17. Briefly, the potency was improved from micromolar to nanomolar with a remarkable increase in ligand efficiency from 0.24 kcal/mol per HAC for the hit **9** to 0.35 kcal/mol per HAC for the derivative **10**. The optimization of both potency and selectivity was based on the favorable polar interactions with the Arg1173 guanidinium of the CREBBP bromodomain as observed in the MD simulations.

In conclusion, both the binding affinity and ligand efficiency of the ALTA hits were improved by the chemical synthesis of a small set of derivatives as in previous applications of the ALTA procedure.[14b,29] MD simulations played a key role, as they provided additional support to the binding mode predicted by docking. Furthermore, the analysis of the interaction motifs along the MD trajectories efficiently guided the hit optimization process.

EXPERIMENTAL SECTION

Preparation of the Fragments for Docking. The fragments used in this study were generated from the molecules in the ZINC leads-now library (version of October 2012) by the program DAIM which carries out an automatic decomposition by cleaving all rotatable bonds.[15] The resulting fragments were parametrized according to the CHARMM general force field (CGenFF)[30] using the program MATCH.[31] About 9% of the fragments were lost in this process because the chemical space is not fully covered by this program yet.

Preparation of the Protein. The atomic coordinates of chain A of the 3P1C and 3SVH PDB files were used. Six of the structured water molecules in the receptor binding pocket (water 1, 2, 3, 4, 6, and 7, as defined in ref 32) were kept for docking. PSFGEN was used to add the missing atoms (including hydrogens). Hydrogen atom positions were minimized with CHARMM[20] using the CHARMM27 force field.

Docking of Fragments. The program SEED (solvation energy for exhaustive docking)[16] was used to dock the fragments. SEED calculates the electrostatic energy using a continuum approximation with an efficient numerical evaluation of the Born radii. These radii approximate the space occupied by the solute (i.e., low-dielectric volume) around individual atoms and are employed in the generalized Born formula for the calculation of the electrostatic contribution to the intermolecular interaction and desolvation of the ligand.[33]

Flexible Docking of the Parent Compounds. The parent compounds of the top 3975 (3SVH) and 4601 (3P1C) fragments were retrieved from the ZINC leads-now library. These were docked to the corresponding CREBBP bromodomain structure using AutoDock Vina.[23] All the poses were then refined via minimization by CHARMM.[20] During minimization the interaction energy between the receptor and the compound was evaluated by the sum of the van der Waals and electrostatic energy. The latter energy was computed with a modified Coulombic term, i.e., distance-dependent dielectric constant ($4.0r$, where r is the distance between partial charges). Then, the poses were filtered by a hydrogen bonding penalty (cutoff 1.0).[21] The remaining compounds were then rescored using the total energy calculated by the program SEED.[16]

The predictive ability of the filtering and scoring of flexible molecules was verified using ROC curves. Seven known inhibitors were used as true positives. ROC curves with AUC values higher than 0.67 were obtained for both structures (Figure S4).

MD Simulations. All MD simulations were carried out by GROMACS 4.6[34] with the CHARMM27/CGenFF force field.[30] The predicted binding poses were used as starting conformations and solvated in cubic water boxes with the TIP3P water model.[35] Long-range electrostatics were treated with the particle mesh Ewald method, while the van der Waals interactions were truncated at a cutoff of 10 Å. After 1 ns of equilibration, production runs were carried out in the *NPT* ensemble at 310 K. The time step was 2 fs, and snapshots were saved for analysis every 20 ps.

Clustering of MD Snapshots and Free-Energy Profile of Binding of Compound 1. A hierarchical tree-based algorithm[36] was used for clustering the coordinate sets saved along the MD simulations. The two 1 μs trajectories were combined, and a total of 50 000 MD snapshots (i.e., one snapshot every 40 ps) were employed for clustering. The RMSD of the ligand heavy atoms and a final fine-grained threshold of 1.0 Å were used for clustering by the tree-based algorithm (with 10 levels of the tree and initial RMSD threshold of 12.0 Å). The tree-based algorithm generated 3929 clusters which were used for calculating the free-energy profile by an automatic procedure which is able to identify all free-energy basins.[27]

Protein Purification and Binding Assays. Protein purification and thermal shift measurements were performed as reported previously.[29b] The description of the competition binding assay and TR-FRET assay is given in the Supporting Information.

ASSOCIATED CONTENT

Supporting Information

General procedures for the fragment docking, synthesis and characterization, and biophysical and biological evaluation of final compounds. The Supporting Information is available free of charge on the ACS Publications website at DOI: 10.1021/acs.jmedchem.5b00171.

Accession Codes

PDB code for CREBBP in complex with the ligand **10** is 4TQN.

AUTHOR INFORMATION

Corresponding Authors

*C.N.: e-mail, cristina.nevado@chem.uzh.ch; phone, +41 44 635 39 45.

*A.C.: e-mail, caflisch@bioc.uzh.ch; phone, +41 44 635 55 21.

Notes

The authors declare no competing financial interest.

ACKNOWLEDGMENTS

We thank Dr. Alvaro Salvador for help with chemical synthesis, and Lisa Caflisch, Lisa Gartenmann, and Lars Wiedmer for help with protein purification and thermal shift assay experiments. We thank the Structural Genomics Consortium at Oxford University for providing the plasmids of the bromodomains. The MD simulations were carried out at the Schrödinger computing cluster of the University of Zurich. This work was supported financially by the Swiss National Science Foundation and the Swiss Cancer League (Krebsliga). D.S. is a recipient of the SystemsX.ch translational postdoc fellowship.

ABBREVIATIONS USED

ALTA, anchor-based library tailoring; AUC, area under the curve; BET, bromodomain and extraterminal; CHARMM, chemistry at Harvard molecular mechanics; CREBBP, CREB binding protein; DMSO, dimethyl sulfoxide; HAC, heavy atom count; MD, molecular dynamics; NMR, nuclear magnetic resonance; RMSD, root-mean-square deviation; ROC, receiver operating characteristic; SEED, solvation energy for exhaustive docking; SEM, standard error of the mean; TR-FRET, time-resolved Förster resonance energy transfer

DOI: 10.1021/acs.jmedchem.5b00171
J. Med. Chem. 2016, 59, 1340−1349

REFERENCES

(1) Sanchez, R.; Meslamani, J.; Zhou, M. M. The bromodomain: from epigenome reader to druggable target. *Biochim. Biophys. Acta, Gene Regul. Mech.* **2014**, *1839*, 676−685.

(2) Filippakopoulos, P.; Knapp, S. The bromodomain interaction module. *FEBS Lett.* **2012**, *586*, 2692−2704.

(3) Filippakopoulos, P.; Picaud, S.; Mangos, M.; Keates, T.; Lambert, J. P.; Barsyte-Lovejoy, D.; Felletar, I.; Volkmer, R.; Muller, S.; Pawson, T.; Gingras, A. C.; Arrowsmith, C. H.; Knapp, S. Histone recognition and large-scale structural analysis of the human bromodomain family. *Cell* **2012**, *149*, 214−231.

(4) (a) Sachchidanand; Resnick-Silverman, L.; Yan, S.; Mutjaba, S.; Liu, W.; Zeng, L.; Manfredi, J. J.; Zhou, M.-M. Target Structure-Based Discovery of Small Molecules that Block Human p53 and CREB Binding Protein Association. *Chem. Biol.* **2006**, *13*, 81−90. (b) Borah, J. C.; Mujtaba, S.; Karakikes, I.; Zeng, L.; Muller, M.; Patel, J.; Moshkina, N.; Morohashi, K.; Zhang, W.; Gerona-Navarro, G.; Hajjar, R. J.; Zhou, M. M. A small molecule binding to the coactivator CREB-binding protein blocks apoptosis in cardiomyocytes. *Chem. Biol.* **2011**, *18*, 531−541.

(5) Gerona-Navarro, G.; Yoel, R.; Mujtaba, S.; Frasca, A.; Patel, J.; Zeng, L.; Plotnikov, A. N.; Osman, R.; Zhou, M. M. Rational design of cyclic peptide modulators of the transcriptional coactivator CBP: a new class of p53 inhibitors. *J. Am. Chem. Soc.* **2011**, *133*, 2040−2043.

(6) Philpott, M.; Yang, J.; Tumber, T.; Fedorov, O.; Uttarkar, S.; Filippakopoulos, P.; Picaud, S.; Keates, T.; Felletar, I.; Ciulli, A.; Knapp, S.; Heightman, T. D. Bromodomain-peptide displacement assays for interactome mapping and inhibitor discovery. *Mol. BioSyst.* **2011**, *7*, 2899−2908.

(7) Hewings, D. S.; Wang, M.; Philpott, M.; Fedorov, O.; Uttarkar, S.; Filippakopoulos, P.; Picaud, S.; Vuppusetty, C.; Marsden, B.; Knapp, S.; Conway, S. J.; Heightman, T. D. 3,5-Dimethylisoxazoles Act As Acetyl-lysine-mimetic Bromodomain Ligands. *J. Med. Chem.* **2011**, *54*, 6761−6770.

(8) Chung, C.-w.; Dean, A. W.; Woolven, J. M.; Bamborough, P. Fragment-Based Discovery of Bromodomain Inhibitors Part 1: Inhibitor Binding Modes and Implications for Lead Discovery. *J. Med. Chem.* **2012**, *55*, 576−586.

(9) Hay, D.; Fedorov, O.; Filippakopoulos, P.; Martin, S.; Philpott, M.; Picaud, S.; Hewings, D. S.; Uttakar, S.; Heightman, T. D.; Conway, S. J.; Knapp, S.; Brennan, P. E. The design and synthesis of 5- and 6-isoxazolylbenzimidazoles as selective inhibitors of the BET bromodomains. *MedChemComm* **2013**, *4*, 140−144.

(10) Hay, D. A.; Fedorov, O.; Martin, S.; Singleton, D. C.; Tallant, C.; Wells, C.; Picaud, S.; Philpott, M.; Monteiro, O. P.; Rogers, C. M.; Conway, S. J.; Rooney, T. P.; Tumber, A.; Yapp, C.; Filippakopoulos, P.; Bunnage, M. E.; Muller, S.; Knapp, S.; Schofield, C. J.; Brennan, P. E. Discovery and Optimization of Small-Molecule Ligands for the CBP/p300 Bromodomains. *J. Am. Chem. Soc.* **2014**, *136*, 9308−9319.

(11) I-CBP112—a CREBBP/EP300-selective chemical probe. http://www.thesgc.org/chemical-probes/ICBP112.

(12) Rooney, T. P.; Filippakopoulos, P.; Fedorov, O.; Picaud, S.; Cortopassi, W. A.; Hay, D. A.; Martin, S.; Tumber, A.; Rogers, C. M.; Philpott, M.; Wang, M.; Thompson, A. L.; Heightman, T. D.; Pryde, D. C.; Cook, A.; Paton, R. S.; Muller, S.; Knapp, S.; Brennan, P. E.; Conway, S. J. A series of potent CREBBP bromodomain ligands reveals an induced-fit pocket stabilized by a cation-pi interaction. *Angew. Chem., Int. Ed.* **2014**, *53*, 6126−6130.

(13) Fedorov, O.; Lingard, H.; Wells, C.; Monteiro, O. P.; Picaud, S.; Keates, T.; Yapp, C.; Philpott, M.; Martin, S. J.; Felletar, I.; Marsden, B. D.; Filippakopoulos, P.; Muller, S.; Knapp, S.; Brennan, P. E. [1,2,4]triazolo[4,3-a]phthalazines: inhibitors of diverse bromodomains. *J. Med. Chem.* **2014**, *57*, 462−476.

(14) (a) Kolb, P.; Kipouros, C. B.; Huang, D.; Caflisch, A. Structure-based tailoring of compound libraries for high-throughput screening: Discovery of novel EphB4 kinase inhibitors. *Proteins: Struct., Funct., Genet.* **2008**, *73*, 11−18. (b) Zhao, H.; Dong, J.; Lafleur, K.; Nevado, C.; Caflisch, A. Discovery of a Novel Chemotype of Tyrosine Kinase Inhibitors by Fragment-Based Docking and Molecular Dynamics. *ACS Med. Chem. Lett.* **2012**, *3*, 834−838.

(15) Kolb, P.; Caflisch, A. Automatic and Efficient Decomposition of Two-Dimensional Structures of Small Molecules for Fragment-Based High-Throughput Docking. *J. Med. Chem.* **2006**, *49*, 7384−7392.

(16) (a) Majeux, N.; Scarsi, M.; Apostolakis, J.; Ehrhardt, C.; Caflisch, A. Exhaustive Docking of Molecular Fragments With Electrostatic Solvation. *Proteins: Struct., Funct., Genet.* **1999**, *37*, 88−105. (b) Majeux, N.; Scarsi, M.; Caflisch, A. Efficient electrostatic solvation model for protein-fragment docking. *Proteins: Struct., Funct., Genet.* **2001**, *42*, 256−268.

(17) Unzue, A.; Xu, M.; Dong, J.; Wiedmer, L.; Spiliotopoulos, D.; Caflisch, A.; Nevado, C. Fragment-Based Design of Selective Nanomolar Ligands of the CREBBP Bromodomain. *J. Med. Chem.* **2015**, DOI: 10.1021/acs.jmedchem.5b00172.

(18) Steiner, S.; Magno, A.; Huang, D.; Caflisch, A. Does bromodomain flexibility influence histone recognition? *FEBS Lett.* **2013**, *587*, 2158−2163.

(19) Chung, C.-w.; Coste, H.; White, J. H.; Mirguet, O.; Wilde, J.; Gosmini, R. L.; Delves, C.; Magny, S. M.; Woodward, R.; Hughes, S. A.; Boursier, E. V.; Flynn, H.; Bouillot, A. M.; Bamborough, P.; Brusq, J.-M. G.; Gellibert, F. J.; Jones, E. J.; Riou, A. M.; Homes, P.; Martin, S. L.; Uings, I. J.; Toum, J.; Clément, C. A.; Boullay, A.-B.; Grimley, R. L.; Blandel, F. M.; Prinjha, R. K.; Lee, K.; Kirilovsky, J.; Nicodeme, E. Discovery and Characterization of Small Molecule Inhibitors of the BET Family Bromodomains. *J. Med. Chem.* **2011**, *54*, 3827−3838.

(20) Brooks, B. R.; Brooks, C. L., 3rd; Mackerell, A. D., Jr.; Nilsson, L.; Petrella, R. J.; Roux, B.; Won, Y.; Archontis, G.; Bartels, C.; Boresch, S.; Caflisch, A.; Caves, L.; Cui, Q.; Dinner, A. R.; Feig, M.; Fischer, S.; Gao, J.; Hodoscek, M.; Im, W.; Kuczera, K.; Lazaridis, T.; Ma, J.; Ovchinnikov, V.; Paci, E.; Pastor, R. W.; Post, C. B.; Pu, J. Z.; Schaefer, M.; Tidor, B.; Venable, R. M.; Woodcock, H. L.; Wu, X.; Yang, W.; York, D. M.; Karplus, M. CHARMM: the biomolecular simulation program. *J. Comput. Chem.* **2009**, *30*, 1545−1614.

(21) Zhao, H.; Huang, D. Hydrogen Bonding Penalty upon Ligand Binding. *PLoS One* **2011**, *6*, e19923.

(22) Filippakopoulos, P.; Knapp, S. Targeting bromodomains: epigenetic readers of lysine acetylation. *Nat. Rev. Drug Discovery* **2014**, *13*, 337−356.

(23) Trott, O.; Olson, A. J. AutoDock Vina: Improving the speed and accuracy of docking with a new scoring function, efficient optimization, and multithreading. *J. Comput. Chem.* **2010**, *31*, 455−461.

(24) (a) Fabian, M. A.; Biggs, W. H., 3rd; Treiber, D. K.; Atteridge, C. E.; Azimioara, M. D.; Benedetti, M. G.; Carter, T. A.; Ciceri, P.; Edeen, P. T.; Floyd, M.; Ford, J. M.; Galvin, M.; Gerlach, J. L.; Grotzfeld, R. M.; Herrgard, S.; Insko, D. E.; Insko, M. A.; Lai, A. G.; Lelias, J. M.; Mehta, S. A.; Milanov, Z. V.; Velasco, A. M.; Wodicka, L. M.; Patel, H. K.; Zarrinkar, P. P.; Lockhart, D. J. A small molecule-kinase interaction map for clinical kinase inhibitors. *Nat. Biotechnol.* **2005**, *23*, 329−336. (b) Quinn, E.; Wodicka, L.; Ciceri, P.; Pallares, G.; Pickle, E.; Torrey, A.; Hunt, J.; Treiber, D. BROMOscan - a high throughput, quantitative ligand binding platform identifies best-in-class bromodomain inhibitors from a screen of mature compounds targeting other protein classes. *Cancer Res.* **2013**, *73*, 4238.

(25) Magno, A.; Steiner, S.; Caflisch, A. Mechanism and Kinetics of Acetyl-Lysine Binding to Bromodomains. *J. Chem. Theory Comput.* **2013**, *9*, 4225−4232.

(26) (a) Lucas, X.; Wohlwend, D.; Hügle, M.; Schmidtkunz, K.; Gerhardt, S.; Schüle, R.; Jung, M.; Einsle, O.; Günther, S. 4-Acyl Pyrroles: Mimicking Acetylated Lysines in Histone Code Reading. *Angew. Chem., Int. Ed.* **2013**, *52*, 14055−14059. (b) Ferguson, F. M.; Fedorov, O.; Chaikuad, A.; Philpott, M.; Muniz, J. R. C.; Felletar, I.; von Delft, F.; Heightman, T.; Knapp, S.; Abell, C.; Ciulli, A. Targeting low druggability bromodomains: Fragment based screening and inhibitor design against the BAZ2B bromodomain. *J. Med. Chem.* **2013**, *56*, 10183−101837.

(27) Blöchliger, N.; Vitalis, A.; Caflisch, A. A scalable algorithm to order and annotate continuous observations reveals the metastable

DOI: 10.1021/acs.jmedchem.5b00171
J. Med. Chem. 2016, 59, 1340−1349

states visited by dynamical systems. *Comput. Phys. Commun.* **2013**, *184*, 2446−2453.
(28) Blöchliger, N.; Vitalis, A.; Caflisch, A. High-resolution visualisation of the States and pathways sampled in molecular dynamics simulations. *Sci. Rep.* **2014**, *4*, 6264.
(29) (a) Lafleur, K.; Huang, D.; Zhou, T.; Caflisch, A.; Nevado, C. Structure-based optimization of potent and selective inhibitors of the tyrosine kinase erythropoietin producing human hepatocellular carcinoma receptor B4 (EphB4). *J. Med. Chem.* **2009**, *52*, 6433−6446. (b) Zhao, H.; Gartenmann, L.; Dong, J.; Spiliotopoulos, D.; Caflisch, A. Discovery of BRD4 bromodomain inhibitors by fragment-based high-throughput docking. *Bioorg. Med. Chem. Lett.* **2014**, *24*, 2493−2496.
(30) Vanommeslaeghe, K.; Hatcher, E.; Acharya, C.; Kundu, S.; Zhong, S.; Shim, J.; Darian, E.; Guvench, O.; Lopes, P.; Vorobyov, I.; Mackerell, A. D. CHARMM general force field: A force field for drug-like molecules compatible with the CHARMM all-atom additive biological force fields. *J. Comput. Chem.* **2010**, *31*, 671−690.
(31) Yesselman, J. D.; Price, D. J.; Knight, J. L.; Brooks, C. L. MATCH: An atom-typing toolset for molecular mechanics force fields. *J. Comput. Chem.* **2012**, *33*, 189−202.
(32) Huang, D.; Rossini, E.; Steiner, S.; Caflisch, A. Structured Water Molecules in the Binding Site of Bromodomains Can Be Displaced by Cosolvent. *ChemMedChem* **2014**, *9*, 573−579.
(33) (a) Scarsi, M.; Apostolakis, J.; Caflisch, A. Continuum Electrostatic Energies of Macromolecules in Aqueous Solutions. *J. Phys. Chem. A* **1997**, *101*, 8098−8106. (b) Scarsi, M.; Apostolakis, J.; Caflisch, A. Comparison of a GB Solvation Model with Explicit Solvent Simulations: Potentials of Mean Force and Conformational Preferences of Alanine Dipeptide and 1,2-Dichloroethane. *J. Phys. Chem. B* **1998**, *102*, 3637−3641.
(34) (a) Hess, B.; Kutzner, C.; van der Spoel, D.; Lindahl, E. GROMACS 4: Algorithms for Highly Efficient, Load-Balanced, and Scalable Molecular Simulation. *J. Chem. Theory Comput.* **2008**, *4*, 435−447. (b) Pronk, S.; Páll, S.; Schulz, R.; Larsson, P.; Bjelkmar, P.; Apostolov, R.; Shirts, M. R.; Smith, J. C.; Kasson, P. M.; van der Spoel, D.; Hess, B.; Lindahl, E. GROMACS 4.5: a high-throughput and highly parallel open source molecular simulation toolkit. *Bioinformatics* **2013**, *29*, 845−854.
(35) Jorgensen, W. L.; Madura, J. D. Quantum and statistical mechanical studies of liquids. 25. Solvation and conformation of methanol in water. *J. Am. Chem. Soc.* **1983**, *105*, 1407−1413.
(36) Vitalis, A.; Caflisch, A. Efficient Construction of Mesostate Networks from Molecular Dynamics Trajectories. *J. Chem. Theory Comput.* **2012**, *8*, 1108−1120.

DOI: 10.1021/acs.jmedchem.5b00171
J. Med. Chem. 2016, 59, 1340−1349